Enhanced polarizability of aromatic molecules placed in the vicinity of silver clusters

Enhanced polarizability of aromatic molecules placed in the vicinity of silver clusters

A Mayer[1,3] and G C Schatz[2]

[1] FUNDP—University of Namur, Rue de Bruxelles 61, B-5000 Namur, Belgium
[2] Northwestern University, 2145 Sheridan Road, Evanston, IL 60208-3113, USA

E-mail: alexandre.mayer@fundp.ac.be

Abstract

We use a charge–dipole interaction model to study the polarizability of aromatic molecules that are placed between two silver clusters. In particular we examine the enhancement in polarizability induced by the clusters at plasmon-like resonant frequencies of the cluster–molecule–cluster system. The model used for these simulations relies on representation of the atoms by both a net electric charge and a dipole. By relating the time variation of the atomic charges to the currents that flow through the bonds of the structures considered, a least-action principle can be formulated that enables the atomic charges and dipoles to be determined. We consider benzene, naphthalene and anthracene for this study, comparing the polarizability of these aromatic molecules when placed in the middle between two Ag_{120} clusters, with their polarizability as isolated molecules. We find that the polarizability of these molecules is enhanced by the clusters, and this increases the electromagnetic coupling between the two clusters. This results in significant red-shifting (by up to 0.8 eV) of the lowest energy optical transition in the cluster–molecule–cluster system compared to plasmon-like excitation in the cluster–cluster system. The resulting resonant polarizability enhancement leads to an electromagnetic enhancement in surface-enhanced Raman scattering of over 10^6.

(Some figures in this article are in colour only in the electronic version)

1. Introduction

The polarization of systems that are subject to external fields is fundamental to the development of new technologies relevant to sensing and electronic/optical devices. Electronic polarization indeed contributes to the dynamics [1–3] or field-induced organization [4, 5] of many complex systems. It is an essential aspect of field emission [6–8], and it enables the determination of macroscopic polarizations [9], hyperpolarizabilities [10–12], Raman intensities [13, 14], etc. In this context, molecular modeling of the polarization properties is commonly achieved with either quantum chemical and classical electrostatics models [15–17]. In molecular mechanics or force field models, electrostatic interactions are for example described using classical models and the trend is to use force fields that include polarization explicitly [18–20].

This enables the polarizability of the structures considered, as well as properties that arise from this polarizability, to be determined.

A classical method to compute molecular polarizabilities consists in associating with each atom a dipole, whose value actually depends on the external field and on the fields associated with the other dipoles [21–27]. An extension of this model consists of associating with each atom an electric charge in addition to the dipole [28–40]. The atomic charges and dipoles are in this case those that minimize the potential energy associated with these quantities, however different models exist for these quantities depending on the expression used for the self-energies and the interactions between different atomic sites. When the external field is oscillating, an approach proposed by others consists in giving the 'monopolar' and 'dipolar' polarizabilities a Lorentzian dependence on the frequency [25, 30, 41–43]. Our approach to this problem

---

[3] Author to whom any correspondence should be addressed.

consists in relating the time variations of the atomic charges to the currents that flow through the bonds of the structure considered [44, 45]. Given appropriate expressions for the kinetic energy of these moving charges, a least-action principle can be formulated that enables the time-dependence of the atomic charges and dipoles to be determined.

Our recent work with this 'charge–dipole model' has focused on the frequency-dependent polarizabilities of aromatic molecules [44] and silver clusters [45] (these structures being considered separately). Silver clusters have attracted wide interest because of their ability to magnify, locally, the fields that are applied to them and because of the enhancement they induce in the Raman scattering of molecules that are placed in their vicinity [46–54]. Of particular interest are cluster–molecule–cluster junction structures, as recent single molecule surface-enhanced Raman spectroscopy (SERS) experiments [55] provide strong evidence that the molecule being observed is always located at such junctions. This has inspired theoretical studies of junctions, including a recent time-dependent-density functional theory study [50] of a junction which consisted of a pyrazine molecule sandwiched between Ag_{20} clusters. Although the silver clusters show plasmon-like optical response that provides a useful model for understanding SERS [53], the Ag_{20}–pyrazine–Ag_{20} structure was found to show only weak electromagnetic coupling between the silver clusters, so the strong electromagnetic coupling that is expected of a junction was not present.

To provide further insight into the uses of the charge–dipole model, it is of interest to apply it to situations in which aromatic molecules and silver clusters are considered simultaneously. Here we consider benzene, naphthalene and anthracene interacting with tetrahedral Ag_{120} clusters as a model of the junction structures noted above, but using larger metal clusters so that electromagnetic interactions between the clusters are stronger. Parameters that can be used in the charge–dipole model were determined in our previous work [44, 45] for these molecules and clusters based on fits to static and frequency-dependent polarizability properties that were obtained from electronic structure calculations. Thus the polarization properties of each component of the junctions are accurately known, and the issue of interest in this work is how interactions between the components influence the overall polarization properties. Note that chemical contributions to the SERS enhancements are not included in this study.

This paper is organized according to the following lines. In section 2, we present the methodology used to simulate the frequency-dependent polarizability of aromatic molecules and silver clusters. In section 3, we compare the polarizability of benzene, naphthalene and anthracene in situations in which these structures are either isolated or placed between two tetrahedral Ag_{120} clusters. The polarizability of these structures turns out to be enhanced by the silver clusters, and this enhances the electromagnetic coupling between the two clusters. This red-shifts the resonant response of the system by surprisingly large amounts (up to 0.8 eV). The dependence of this resonance on the distance between the two clusters, and the magnitudes of the resonance SERS enhancement factor are then used to provide insight concerning which junction

structures are likely to play a role in SERS. Our conclusions are presented in section 4.

2. Methodology

We summarize in this section the methodology presented in our previous work for the calculation of frequency-dependent polarizabilities using the charge–dipole model. We consider a system of N atoms, which are split into N_S structures. By 'structures', we refer to chemically stable sets of atoms and we will assume that charge transfers are allowed only between the atoms of a given structure. Charge transfers between different structures are hence prevented in this work. The structures considered later in this paper are benzene, naphthalene, anthracene and tetrahedral Ag_{120} clusters. We refer by Q_{tot}^k to the net charge carried by each structure ($k \in [1, N_S]$). We assume that these structures are subject to an external field, whose time-dependence is given by $\mathbf{E}_{ext}(t) = \text{Re}[\mathbf{E}_{ext} \exp(-i\omega t)]$, where $\mathbf{E}_{ext}$ stands for the amplitude of this external field and ω for its angular frequency. We associate with each atom a net electric charge $q_i(t)$ as well as a dipole $\mathbf{p}_i(t)$. These quantities are expressed as $q_i(t) = q_i^0 + \text{Re}[q_i \exp(-i\omega t)]$ and $\mathbf{p}_i(t) = \mathbf{p}_i^0 + \text{Re}[\mathbf{p}_i \exp(-i\omega t)]$, where q_i and $\mathbf{p}_i$ refer to the complex amplitude of the oscillating part of $q_i(t)$ and $\mathbf{p}_i(t)$. q_i^0 and $\mathbf{p}_i^0$ refer to the steady part of $q_i(t)$ and $\mathbf{p}_i(t)$. The charge-specification conditions are expressed as $\sum_i f_k^i q_i^0 = Q_{tot}^k$ and $\sum_i f_k^i q_i = 0$, where $f_k^i = 1$ if the atom i belongs to the structure k and $f_k^i = 0$ otherwise. We will consider neutral structures in this paper, so that $Q_{tot}^k = 0$.

The potential energy of this distribution of charges and dipoles is given by

$$
\begin{aligned}
E_{pot}(t) = & \frac{1}{2} \sum_{i=1}^{N} \sum_{j=1}^{N} q_i(t) T_{q-q}^{i,j} q_j(t) \\
& - \frac{1}{2} \sum_{i=1}^{N} \sum_{j=1}^{N} \mathbf{p}_i(t) \cdot \mathbf{T}_{p-p}^{i,j} \mathbf{p}_j(t) \\
& - \sum_{i=1}^{N} \sum_{j=1}^{N} \mathbf{p}_i(t) \cdot \mathbf{T}_{p-q}^{i,j} q_j(t) \\
& + \sum_{i=1}^{N} q_i(t)[\chi_i + V_i(t)] - \sum_{i=1}^{N} \mathbf{p}_i(t) \cdot \mathbf{E}_{ext}(t), \quad (1)
\end{aligned}
$$

where $T_{q-q}^{i,j}$, $\mathbf{T}_{p-p}^{i,j}$ and $\mathbf{T}_{p-q}^{i,j}$ express respectively the charge–charge, the dipole–dipole and the charge–dipole interactions. χ_i refers to the absolute electronegativity of the atom i and $V_i(t) = -\mathbf{E}_{ext}(t) \cdot \mathbf{r}_i$ is the potential associated with the external field $\mathbf{E}_{ext}(t)$ at the atomic position $\mathbf{r}_i$. This expression actually depends, through the on-site terms $T_{q-q}^{i,i}$ and $\mathbf{T}_{p-p}^{i,i}$ and through the normalization of the electrostatic interactions, on the extension R_q^i of the atomic charges and on the atomic polarizabilities α_i [37, 38, 44].

In order to express the kinetic energy of the moving charges, we relate the time variations of the atomic charges $q_i(t)$ to the currents $I_l(t)$ that flow through the bonds of the structures considered. This relation $I_l(t) = \sum_{i=1}^{N} A_{l,i} \dot{q}_i$ is actually established by enforcing (i) that the time variation of the atomic charges be equal to the sum of the incoming

currents (for each atom and considering the currents that flow through the bonds of this atom), and (ii) that no potential difference exists when going along any closed path [45]. One can then express the kinetic energy of the moving charges as $E_{\text{kin,q}}(t) = \sum_{l=1}^{N_{\text{bonds}}} R_l [\sum_{i=1}^{N} A_{l,i} \dot{q}_i(t)]^2$, where the sum runs over the N_{bonds} bonds of the structures considered. The coefficients R_l express the 'resistance' of each bond. We express it as $R_l = c_{\text{kin,q}} \frac{m}{2e^2} \frac{d_l^2}{S_l}$, where $c_{\text{kin,q}}$ is a proportionality coefficient, m is the mass of the electron, e is the electronic charge, and d_l is the length of the bond l. S_l refers to the overlap between the normalized Gaussian distributions that are associated with the two atoms that are connected by the bond l in order to express their contribution to the resistance R_l. For silver clusters, S_l actually depends on the extension R_c^i of these distributions, which are specific to each type of atom [45]. For the aromatic molecules studied in [44], it was not necessary to introduce differences between the bonds that contribute to the charge transfers. This comes to enforcing $S_l = 1$ for these structures. The kinetic energy of the oscillating dipoles is finally given by $E_{\text{kin,p}}(t) = \frac{m}{2e^2} \sum_{i=1}^{N} c_{\text{kin,p}}^i \dot{\mathbf{p}}_i^2(t)$, where $c_{\text{kin,p}}^i$ is another proportionality coefficient that is specific to each type of atom [45].

Given these expressions for $E_{\text{pot}}(t)$, $E_{\text{kin,q}}(t)$ and $E_{\text{kin,p}}(t)$ and taking account of the constrains associated with the charge Q_{tot}^k carried by each structure, the action J to be minimized is given by

$$J = \int \left\{ L[q_i(t), \dot{q}_i(t), \mathbf{p}_i(t), \dot{\mathbf{p}}_i(t)] - \sum_{k=1}^{N_S} \lambda_k \left[\sum_{i=1}^{N} f_k^i q_i(t) - Q_{\text{tot}}^k \right] \right\} dt, \quad (2)$$

where $L = (E_{\text{kin,q}} + E_{\text{kin,p}}) - E_{\text{pot}}$ is the Lagrangian and λ_k is the Lagrange multiplier associated with the charge-specification conditions [56]. The formulation of the least-action principle ($\delta J = 0$) finally leads to two sets of $4N + N_S$ linear equations that enable the q_i^0, $\mathbf{p}_i^0$, q_i, $\mathbf{p}_i$ as well as the Lagrange multipliers to be determined [44, 45].

The frequency-independent terms q_i^0 and $\mathbf{p}_i^0$ do not depend on the external field and rather describe the permanent polarization of the structures considered [38, 44]. For the calculation of molecular polarizabilities, one only needs the complex amplitude q_i and $\mathbf{p}_i$ of the oscillating part of the atomic charges and dipoles [44, 45]. Their values are provided by the matricial equation

$$\begin{pmatrix} \mathbf{T}_{\text{q-q}} - \omega^2 \mathbf{K}_{\text{q-q}} & -\mathbf{T}_{\text{q-p}} & \mathbf{F} \\ -\mathbf{T}_{\text{p-q}} & -\mathbf{T}_{\text{p-p}} - \omega^2 \mathbf{K}_{\text{p-p}} & \mathbf{0} \\ \mathbf{F}^t & \mathbf{0} & \mathbf{0} \end{pmatrix} \begin{pmatrix} \mathbf{q} \\ \mathbf{p} \\ \boldsymbol{\lambda} \end{pmatrix}$$
$$= \begin{pmatrix} -\mathbf{V} \\ \mathbf{E} \\ \mathbf{0} \end{pmatrix}, \quad (3)$$

where $\mathbf{q}$, $\mathbf{p}$ and $\boldsymbol{\lambda}$ are vectors of size N, $3N$ and N_S that contain respectively the q_i, the components of the $\mathbf{p}_i$ and the Lagrange multipliers associated with the conditions $\sum_i f_k^i q_i = 0$. $\mathbf{T}_{\text{q-q}}$, $\mathbf{T}_{\text{p-q}}$ and $\mathbf{T}_{\text{p-p}}$ contain the $T_{\text{q-q}}^{i,j}$, $T_{\text{p-q}}^{i,j}$ and $T_{\text{p-p}}^{i,j}$. $\mathbf{T}_{\text{q-p}} = \mathbf{T}_{\text{p-q}}^t$. $\mathbf{F}$ contains the f_k^i. $\mathbf{K}_{\text{q-q}} = 2\mathbf{A}^t\mathbf{R}\mathbf{A}$, with $\mathbf{A}$ the matrix that contains the $A_{l,i}$ and $\mathbf{R}$ a diagonal matrix that contains the
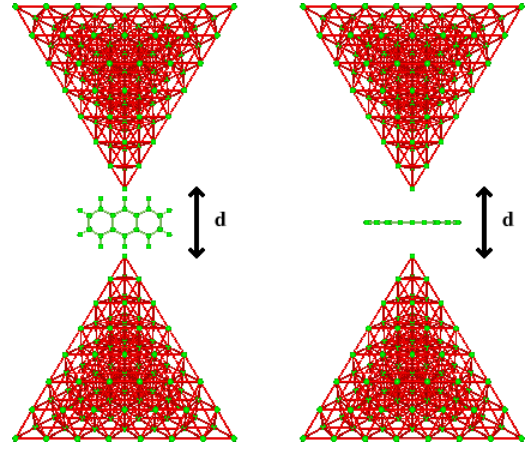

Figure 1. Anthracene placed between two tetrahedral Ag$_{120}$ clusters placed tip-to-tip with a gap distance d of 7 Å. The left and right parts of the figure represent the molecule in respectively a vertical and horizontal position.

R_l. $\mathbf{K}_{\text{p-p}}$ is a diagonal matrix that contains the $\frac{m}{e^2} c_{\text{kin,p}}^i$. $\mathbf{V}$ and $\mathbf{E}$ contain respectively the V_i and the components of the external field $\mathbf{E}_{\text{ext}}$ on each atom. Dissipation is finally introduced by replacing $\omega^2 \mathbf{K}_{\text{q-q}}$ by $(\omega^2 + i\gamma_q\omega)\mathbf{K}_{\text{q-q}}$ and $\omega^2 \mathbf{K}_{\text{p-p}}$ by a diagonal matrix with elements given by $(\omega^2 + i\gamma_p^i\omega)\frac{m}{e^2} c_{\text{kin,p}}^i$, where $\gamma_q = 1/\tau_q$ and $\gamma_p^i = 1/\tau_p^i$ are damping parameters. The parameters that enable the modeling of aromatic molecules and silver clusters come respectively from [44] and [45]. They are given in table 1. An implementation of this methodology is provided by the DCDA software [57].

3. Application: polarization properties of aromatic molecules that are placed in the middle between two silver clusters

In order to study the enhancement that silver clusters can induce on the polarizability of molecules that are placed in their vicinity, we considered situations in which benzene, naphthalene and anthracene are placed in the middle between two tetrahedral Ag$_{120}$ clusters. We will assume that each molecule and each cluster has a net charge $Q_{\text{tot}}^k = 0$. We prevent in this study any transfer of charges between the aromatic molecules and the silver clusters. We assume that these clusters are placed 'tip-to-tip' along the z-axis, with a gap distance d between the apex of each cluster. We will consider situations in which the aromatic molecules are either in a 'vertical' or 'horizontal' position. These denominations refer to situations in which the aromatic molecules are respectively in the xz or xy plane. These two situations are depicted in figure 1.

We consider first the case in which the external field is static and we focus on the molecular polarizability $\boldsymbol{\alpha}$ of the aromatic molecule that is placed between the two clusters. This quantity is defined by the relation

$$\mathbf{P} = \sum_{i \in \text{molec}} (q_i \mathbf{r}_i + \mathbf{p}_i) = \boldsymbol{\alpha} \mathbf{E}_{\text{ext}}, \quad (4)$$

Table 1. Parameters used for the representation of the tetrahedral Ag_{120} clusters and for the representation of aromatic molecules. Bulk Ag atoms are defined as silver atoms that are surrounded by twelve first-neighbor atoms within the cluster, while surface Ag atoms are surrounded by a smaller number of atoms. For silver, the bond resistances R_l are calculated using $R_l = c_{\mathrm{kin,q}} \frac{m}{2e^2} \frac{d_l^2}{S_l}$ with S_l calculated according to the values of R_c [45]. The atomic polarizabilities are isotropic. For aromatic molecules, the bond resistances R_l are calculated using $R_l = c_{\mathrm{kin}}^{\mathrm{q}} \frac{m}{2e^2} d_l^2$ so that the parameter R_c is not used. α_{par} refers in this case to the component of the polarizability tensor in the plane defined by the three neighbors of each atom, while α_{perp} refers to the component of the polarizability tensor in the direction perpendicular to that plane [44].

Ag_{120}	R_q (Å)	$\alpha_{\mathrm{iso}}/(4\pi\epsilon_0)$ (Å^3)	R_c (Å)	$c_{\mathrm{kin,p}}$	γ_p (10^{15} s^{-1})
Ag (bulk)	3.3626	1.8789	7.9080	2.6789	1.0293
Ag (surface)	1.1853	1.0821	0.9532	3.5891	1.1326
$c_{\mathrm{kin,q}} = 0.9831$ nm^{-3}					
$\gamma_q = 0.198\,05 \times 10^{15}$ s^{-1}					

Aromatic molecules	R_q (Å)	$\alpha_{\mathrm{par}}/(4\pi\epsilon_0)$ (Å^3)	$\alpha_{\mathrm{perp}}/(4\pi\epsilon_0)$ (Å^3)	$c_{\mathrm{kin,p}}$	γ_p (10^{15} s^{-1})
Hydrogen	0	0.3057	0.3057	0	0
Carbon	0.022 79	1.4755	2.2611	1.7560	3.6077
$c_{\mathrm{kin}}^{\mathrm{q}} = 9.3026$					
γ_q and R_c not used					

where the summation only includes the atoms that belong to the molecule. **P** is the polarization induced by the external field $\mathbf{E}_{\mathrm{ext}}$. Since the relation $\sum_{i\in\mathrm{molec}} q_i = 0$ holds, **P** is independent of any particular choice for the origin. We compute $\boldsymbol{\alpha}$ by applying an external field $\mathbf{E}_{\mathrm{ext}}$ successively in the x, y and z directions. The polarizability **P** divided by the amplitude of the external field $\mathbf{E}_{\mathrm{ext}}$ provides respectively the first, second and third row of the polarizability tensor $\boldsymbol{\alpha}$. The enhancement of the polarizability of the molecule that is placed between the two clusters is the most significant along the z axis of the dimer. We will therefore focus on the α_{zz} component of the polarizability tensor.

In figure 2, we calculated the ratio between the α_{zz} values obtained when the molecule is placed between the two clusters and the α_{zz} values obtained when the molecule is isolated. These results are established for a gap distance d between the two clusters that ranges between 7 and 40 Å and for either a vertical or an horizontal position of the molecule. Figure 2 shows that the enhancement induced by the silver clusters on the α_{zz} component of the static polarizability tensor of the molecules considered is stronger at smaller gap distances d. It tends as expected to a value of 1 when $d \to \infty$. The enhancement in the values of α_{zz} turns out to be more pronounced when the molecule is in a vertical position (compared to the enhancement achieved for an horizontal position). We will show hereafter that the molecule actually enhances the electromagnetic coupling between the two clusters. This enhancement, which is more significant when the molecule is in a vertical position, contributes to the larger values of α_{zz}.

In [45], we calculated the $E_{\mathrm{middle}}/E_{\mathrm{ext}}$ ratio between the electric field E_{middle} in the middle of the gap and the field E_{ext} that is applied to the dimer. For a gap distance d of 7 Å and without any molecule being placed between the two clusters, this $E_{\mathrm{middle}}/E_{\mathrm{ext}}$ ratio takes the value of 4.5. For aromatic molecules that are placed in a vertical position, the enhancement in the values of α_{zz} turns out be larger than this $E_{\mathrm{middle}}/E_{\mathrm{ext}}$ ratio (actually for the whole range of gap distances d considered). This enhancement in the values of
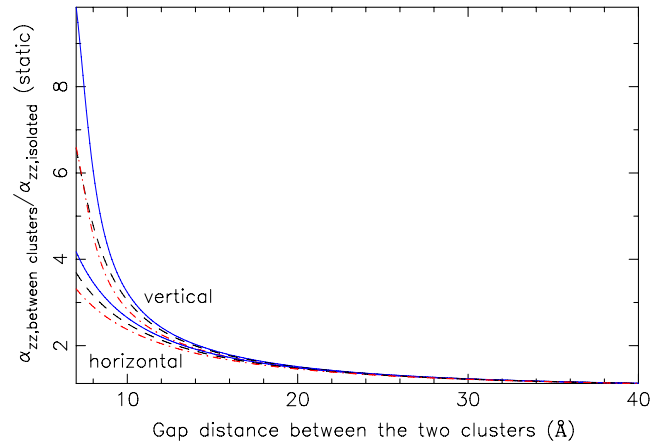

Figure 2. Ratio between the α_{zz} component of the static polarizability of benzene (solid), naphthalene (dashed) and anthracene (dot–dashed) when placed in the middle between two Ag_{120} clusters and the α_{zz} values obtained when these molecules are isolated. The molecules are in a vertical or horizontal position (downwards, as indicated). The results are calculated as a function of the gap distance d between the two clusters.

α_{zz} is however smaller than the $E_{\mathrm{middle}}/E_{\mathrm{ext}}$ ratio achieved when the molecule is in an horizontal position. We note also that the enhancement in the values of α_{zz} is more significant for smaller molecules, like benzene. This may be due to the fact the field that these smaller molecules experience is on average larger than that experienced by larger molecules (the smaller molecules fit indeed better than the larger molecules in the region between the two clusters where the fields are the strongest).

These results are relevant to the molecule that is placed between the two clusters and the polarizabilities presented are those defined by equation (4). Another possibility to quantify the enhancement that occurs in the polarizability of the Ag_{120}–molecule–Ag_{120} system consists in calculating $\Delta\boldsymbol{\alpha} = \boldsymbol{\alpha}_{Ag_{120}-\mathrm{mol}-Ag_{120}} - \boldsymbol{\alpha}_{Ag_{120}-Ag_{120}} - \boldsymbol{\alpha}_{\mathrm{mol}}$, where $\boldsymbol{\alpha}_{Ag_{120}-\mathrm{mol}-Ag_{120}}$ is the polarizability of the entire Ag_{120}–molecule–Ag_{120} system,

Table 2. Comparison between the zz-component of the static polarizability tensor of (i) the entire Ag_{120}–molecule–Ag_{120} system ($\alpha_{zz,Ag-mol-Ag}$), (ii) the Ag_{120}–Ag_{120} dimer ($\alpha_{zz,Ag-Ag}$), (iii) the isolated molecule ($\alpha_{zz,mol}$), (iv) the difference $\Delta\alpha_{zz} = \alpha_{zz,Ag-mol-Ag} - \alpha_{zz,Ag-Ag} - \alpha_{zz,mol}$, and (v) the molecule when placed between the two clusters ($\alpha_{zz,mol\ in\ Ag-mol-Ag}$). This last quantity is calculated according to equation (4) in the text. The molecule consists of either benzene, naphthalene and anthracene, in either a vertical or horizontal position, as indicated. The gap distance d between the two clusters is 7 Å.

	$\frac{\alpha_{zz,Ag-mol-Ag}}{4\pi\epsilon_0}$ ($Å^3$)	$\frac{\alpha_{zz,Ag-Ag}}{4\pi\epsilon_0}$ ($Å^3$)	$\frac{\alpha_{zz,mol}}{4\pi\epsilon_0}$ ($Å^3$)	$\frac{\Delta\alpha_{zz}}{4\pi\epsilon_0}$ ($Å^3$)	$\frac{\alpha_{zz,mol\ in\ Ag-mol-Ag}}{4\pi\epsilon_0}$ ($Å^3$)
			Vertical		
Benzene	2415.13	1786.06	11.92	617.15	117.29
Naphthalene	2329.40	1786.06	17.86	525.47	117.35
Anthracene	2529.28	1786.06	23.65	719.56	155.91
			Horizontal		
Benzene	1877.40	1786.06	5.64	85.71	23.53
Naphthalene	1897.80	1786.06	8.53	103.22	31.46
Anthracene	1911.09	1786.06	11.41	113.63	37.82

$\boldsymbol{\alpha}_{Ag_{120}-Ag_{120}}$ is the polarizability of the Ag_{120}–Ag_{120} dimer when no molecule is placed between the two clusters and $\boldsymbol{\alpha}_{mol}$ is the polarizability of the molecule when the silver clusters are not present. We always assume that the molecule and the two Ag_{120} clusters have a net charge $Q_{tot}^k = 0$ and that no charge transfer occurs between these different structures. We focus as previously on the zz-component of these polarizabilities. The results achieved when a gap distance d of 7 Å is considered are presented in table 2. The values achieved for $\Delta\alpha_{zz}$ confirm that the molecule that is placed between the two clusters induces an enhancement in the polarizability of the Ag_{120}–molecule–Ag_{120} system. This enhancement is larger when the molecule is in a vertical position. These values of $\Delta\alpha_{zz}$ describe the enhancement that occurs in the polarizability of the entire Ag_{120}–molecule–Ag_{120} system when the molecule and the dimer are taken together. $\Delta\alpha_{zz}$ therefore also includes the enhancement that occurs in the polarizability of the Ag_{120}–Ag_{120} dimer. In contrast, the α_{zz} values obtained from equation (4) are only relevant to the molecule that is placed between the two clusters. The remaining part of this paper uses the definition of α_{zz} provided by equation (4). These results are relevant to the off-resonant change in intensities associated with surface-enhanced Raman scattering.

In our previous work [45], we presented calculations of the frequency-dependent polarizability $\boldsymbol{\alpha}(\omega)$ of dimers of silver clusters [40, 46–54]. The imaginary part of the polarizability tensor is characterized by peak intensities, whose displacements (when the gap distance d is changed) are representative of their electromagnetic coupling. It is therefore interesting to study the impact of the aromatic molecules on the position of these peaks. We represented in figure 3 the imaginary part of the polarizability $\boldsymbol{\alpha}(\omega)$ of a Ag_{120}–Ag_{120} dimer, for a gap distance d of 7 Å and for $\hbar\Omega$ values ranging between 1.5 and 3.5 eV. The imaginary part of the α_{xx} and α_{yy} components is characterized by a peak intensity, whose position is blue-shifted from $\hbar\omega = 3.048$ eV (value obtained for an isolated Ag_{120}) to a value of 3.054 eV (these components of the polarizability tensor are associated with a transverse polarization of the dimer) [45, 50]. The imaginary part of the α_{zz} component is also characterized by a peak intensity, whose position is this time red-shifted from $\hbar\omega = 3.048$ eV to
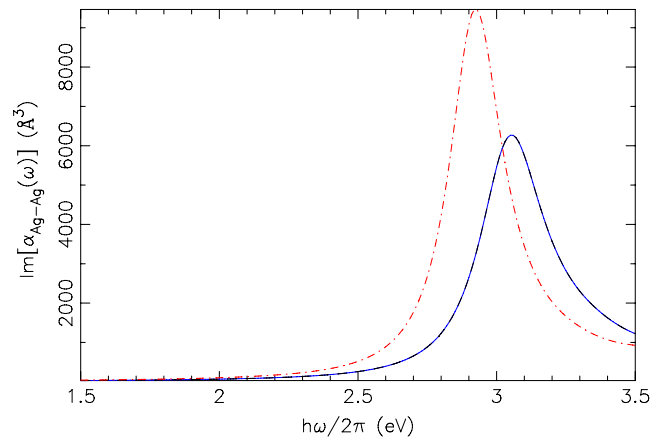

Figure 3. Imaginary part of the polarizability of a Ag_{120}–Ag_{120} dimer. The solid, dashed and dot–dashed lines correspond respectively to the α_{xx}, α_{yy} and α_{zz} components. The gap distance d between the two clusters is 7 Å.

a value of 2.924 eV (this component of the polarizability tensor is associated with an axial polarization of the dimer) [45, 50].

The presence of an aromatic molecule between the two clusters increases the magnitude of this effect. This is illustrated in figure 4, where we represented the imaginary part of the polarizability $\boldsymbol{\alpha}(\omega)$ of a Ag_{120}–anthracene–Ag_{120} system, for a gap distance d of 7 Å and for $\hbar\Omega$ values ranging between 1.5 and 3.5 eV. The figure compares the results achieved when the molecule is either in a vertical or an horizontal position. The peak intensities associated with the α_{xx} and α_{yy} components of the polarizability tensor $\boldsymbol{\alpha}(\omega)$ are hardly affected by the presence of anthracene. In contrast, the peak associated with the α_{zz} component of the polarizability tensor of the Ag_{120}–anthracene–Ag_{120} system is significantly affected by the presence of anthracene. For a vertical position of this molecule, the peak in the $Im[\alpha_{zz}(\omega)]$ data is moved to $\hbar\omega = 2.207$ eV. This corresponds to a red-shift of 0.841 eV compared to the value of 3.048 eV obtained with an isolated Ag_{120}. For an horizontal position of anthracene, the peak in the $Im[\alpha_{zz}(\omega)]$ data is moved to $\hbar\omega = 2.845$ eV (red-shift of 0.203 eV compared to the peak at 3.048 eV). These red-

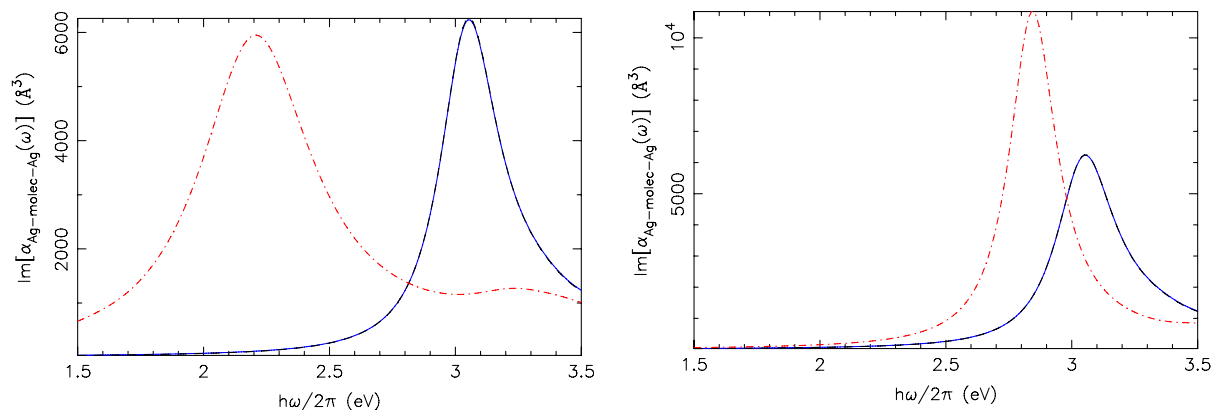**Figure 4.** Imaginary part of the polarizability of a Ag_{120}–anthracene–Ag_{120} system. The solid, dashed and dot–dashed lines correspond respectively to the α_{xx}, α_{yy} and α_{zz} components. Anthracene is either in a vertical (left) or horizontal (right) position. The gap distance d between the two clusters is 7 Å.

shifts of 0.841 eV (for a vertical position) and 0.203 eV (for an horizontal position) are larger than the value of 0.124 eV obtained for the same gap distance d but without anthracene. The presence of an aromatic molecule between the two silver clusters enhances therefore the splitting between the peak intensities in the imaginary part of $\boldsymbol{\alpha}(\omega)$. This can again be interpreted by an enhancement of the coupling between the two clusters, which is indeed more pronounced when the aromatic molecule is in a vertical position.

The polarization of the Ag_{120}–Ag_{120} system induces polarization in anthracene and the frequency-dependence of the polarizability of this molecule tracks that of the complete system. This is illustrated in figure 5, where we show the imaginary part of the α_{zz} component of the polarizability tensor of anthracene, for a vertical and horizontal position of this molecule in the Ag_{120}–anthracene–Ag_{120} system. These $Im[\alpha_{zz}(\omega)]$ data are characterized by a peak intensity for $\hbar\omega = 2.188$ eV when the molecule is vertical and $\hbar\omega = 2.841$ eV when the molecule is horizontal. These values are very close to positions of 2.207 and 2.845 eV that characterize the polarizability of the complete system (for the two orientations of the molecule). The position of these peaks actually depends on the gap distance d between the two clusters and it appears therefore that this parameter can be used to control the frequency at which the molecule has a resonant polarization. Since this polarization determines in turn the Raman scattering intensities this molecule may provide and because of the importance of this technique, we focused the remaining part of this paper on the polarizability of the molecules that are placed between the two clusters.

In figure 6, we represent the energy of the peak intensities of the imaginary part of the α_{zz} component of the polarizability of benzene, naphthalene and anthracene when these molecules are placed between two Ag_{120} clusters. The results are presented as a function of the gap distance d between the two clusters and we consider that the aromatic molecules are either in a vertical or horizontal position. The representation also includes the peak-intensity energies of the α_{zz} component of the polarizability of the Ag_{120}–Ag_{120} dimer (without any molecule placed between the two clusters). The results show
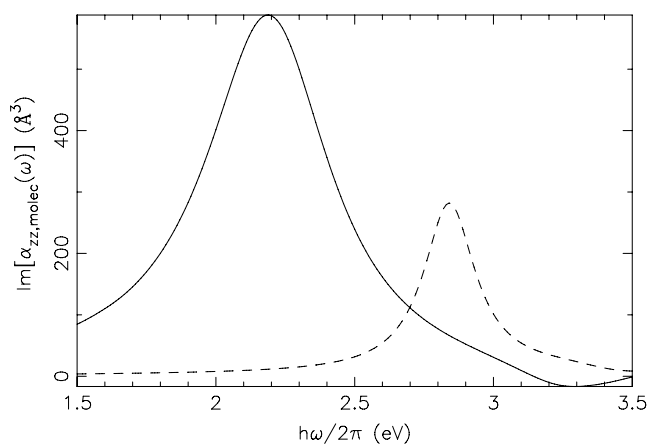

Figure 5. Imaginary part of the α_{zz} component of the polarizability of anthracene in a Ag_{120}–anthracene–Ag_{120} system. The solid and dashed lines correspond respectively to a vertical and horizontal position of the molecule. The gap distance d between the two clusters is 7 Å.

that the peak-intensity energies of the $Im[\alpha_{zz}]$ data are moved to energies that are systematically smaller than those achieved with the Ag_{120}–Ag_{120} dimer. This indicates again that the coupling between the two clusters is enhanced by the aromatic molecule that is placed in-between. The red-shifts achieved when the molecule is in a vertical position are larger in magnitude than those achieved when the molecule is in an horizontal position (we obtain red-shifts up to 0.859 eV for a vertical position of anthracene and a gap distance d of 7 Å, while a value of 0.207 eV is achieved for an horizontal position). The similarity between the results achieved for benzene, naphthalene and anthracene indicates that these peak-intensity energies are essentially determined by the silver clusters and that the aromatic molecule merely enhances the coupling between these clusters. In the limit when $d \rightarrow \infty$, we tend to the value of 3.048 eV obtained for an isolated Ag_{120} cluster.

Finally, in figure 7, we show the ratio between the α_{zz} component of the polarizability at resonance of benzene,
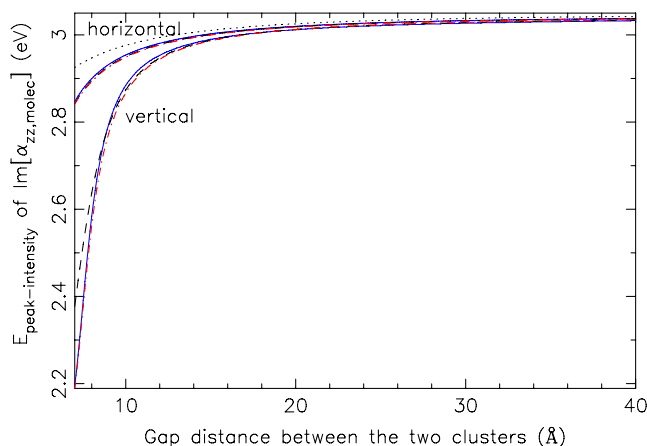
Figure 6. Peak-intensity energies of the imaginary part of the α_{zz} component of the polarizability of benzene (solid), naphthalene (dashed) and anthracene (dot–dashed) when these structures are placed in the middle between two Ag$_{120}$ clusters. The molecules are in a vertical or horizontal position (upwards, as indicated). The results are calculated as a function of the gap distance d between the two clusters. The dotted line indicates the peak-intensity energies of the Ag$_{120}$–Ag$_{120}$ dimer (without any molecule placed between the two clusters).

Figure 7. Ratio between the α_{zz} component of the polarizability at resonance of benzene (solid), naphthalene (dashed) and anthracene (dot–dashed) when placed in the middle between two Ag$_{120}$ clusters and the α_{zz} values obtained when these molecules are isolated. These polarizabilities are calculated for the peak-intensity energies of figure 6. The molecules are in a vertical or horizontal position (downwards, as indicated).

naphthalene and anthracene when these molecules are placed between the two clusters and the α_{zz} values obtained when these molecules are isolated (these α_{zz} values are calculated for the peak-intensity energies $\hbar\omega_{res}$ given in figure 6). This ratio actually represents the enhancement induced by the silver clusters on the α_{zz} component of the polarizability of these molecules (for the frequencies ω_{res} provided by figure 6). Compared to the enhancements obtained in the static case (see figure 2), the enhancements achieved at resonance turn out to be larger by a typical factor of five. For benzene, the silver clusters are actually responsible for an enhancement of the α_{zz} component of its polarizability by a factor of 46.6 (compared to the value obtained when this molecule is isolated). This enhancement is achieved considering a vertical position of benzene and a gap distance d of 7 Å. For comparison, an enhancement of 19.7 is obtained when benzene is in an horizontal position. The enhancements achieved for a vertical position turn out to be systematically larger than those achieved for an horizontal position of the molecule considered. One can finally compare these enhancements in the polarizability with the E_{middle}/E_{ext} ratio obtained at resonance for the Ag$_{120}$–Ag$_{120}$ dimer (when no molecule is placed between the two clusters). For the same gap distance d of 7 Å, one obtains a E_{middle}/E_{ext} ratio of 36.7, which is comparable with the enhancements achieved in the polarizability of the structures placed between the two clusters (when vertical positions are considered).

These results show that the polarizability of molecules that are placed in the vicinity of silver clusters is enhanced compared to the values obtained when they are isolated. This enhancement is the most significant at frequencies for which a resonant polarization of the Ag–molecule–Ag system is achieved. The enhancement factor can then reach values as high as forty when the distance to the clusters is sufficiently
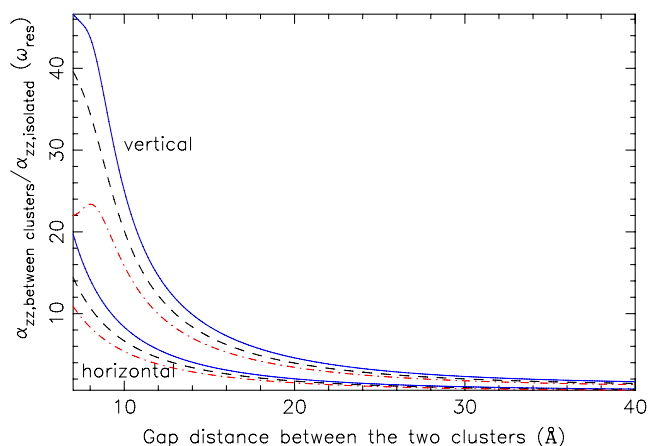
small. This corresponds to surface-enhanced Raman scattering (SERS) enhancement factors of the order of 2.5×10^6, which is the typical order of magnitude expected for SERS [50, 51, 45], although it is lower than what is obtained for electromagnetic theory estimates for junction structures based on 50 nm nanoparticles [55]. Most likely, it will be necessary to use larger clusters to obtain enhancement factors that more accurately mimic what is found in the experiments. This may also influence the dependence of the enhancement factors on gap distance, including the frequency-dependence of the resonance enhancements.

4. Conclusion

We used a charge–dipole interaction model to study the frequency-dependent polarizability of aromatic molecules that are placed between two silver clusters. The results show that the polarization of these molecules is enhanced by the silver clusters. These molecules in turn enhance the electromagnetic coupling between the two clusters. These effects are more pronounced when the molecule is in a vertical position (in contrast with an horizontal position perpendicular to the axis of the dimer). The enhancement in the coupling between the two clusters increases the displacements of the peak intensities of the imaginary part of the polarizability of the Ag-molecule-Ag system (especially for the component of this polarizability that is associated with polarization along the axis of the dimer). The frequency-dependence of the polarizability of the molecule that is placed between the two clusters turns out to follow that of the complete system and a resonance in this polarizability is induced by the dimer. The frequency at which this resonant polarization occurs depends on the gap distance between the two clusters. This gap distance could therefore be used to control the frequency at which molecules that are placed between two silver clusters are most sensitive to an

external field. In particular, for SERS applications, significant enhancements are expected for particle gaps below 1 nm. This will be developed with more details in future work.

Acknowledgments

References

[1] Engkvist O, Åstrand P-O and Karlström G 2000 *Chem. Rev.* **100** 4087
[2] Rick S W and Stuart S J 2002 *Rev. Comput. Chem.* **18** 89
[3] Moulin F, Devel M and Picaud S 2005 *Phys. Rev.* B **71** 165401
[4] Stern H A, Rittner F, Berne B J and Friesner R A 2001 *J. Chem. Phys.* **115** 2237
[5] Mayer A and Lambin Ph 2005 *Nanotechnology* **16** 2685
[6] Mayer A and Vigneron J P 1999 *Ultramicroscopy* **79** 35
[7] Mayer A, Chung M S, Weiss B L, Miskovsky N M and Cutler P H 2008 *Phys. Rev.* B **77** 085411
[8] Mayer A, Chung M S, Weiss B L, Miskovsky N M and Cutler P H 2008 *Phys. Rev.* B **78** 205404
[9] Jensen L, Åstrand P-O and Mikkelsen K V 2004 *J. Phys. Chem.* B **108** 8226
[10] Sundberg K R 1977 *J. Chem. Phys.* **66** 114
[11] Jensen L, Sylvester-Hvid K O, Mikkelsen K V and Åstrand P-O 2003 *J. Phys. Chem.* A **107** 2270
[12] Jensen L, Astrand P-O and Mikkelsen K V 2009 *J. Comput. Theor. Nanosci.* **6** 270
[13] Bocian D F, Schick G A and Birge R R 1981 *J. Chem. Phys.* **74** 3660
[14] Janesko B G and Scuseria G E 2006 *J. Chem. Phys.* **125** 124704
[15] Kanis D R, Ratner M A and Marks T J 1994 *Chem. Rev.* **94** 195
[16] Brédas J L, Adant C, Tackx P, Persoons A and Pierce B M 1994 *Chem. Rev.* **94** 243
[17] Bishop D M and Norman P 2000 *Handbook of Advanced Electronic and Photonic Materials* (San Diego, CA: Academic)
[18] Kaminski G A, Stern H A, Berne B J, Friesner R A, Cao Y X, Murphy R B, Zhou R and Halgren T A 2002 *J. Comput. Chem.* **23** 1515
[19] Ponder J W and Case D A 2003 *Adv. Protein Chem.* **66** 27
[20] Yu H and van Gunsteren W F 2005 *Comput. Phys. Commun.* **172** 69
[21] Silberstein L 1917 *Phil. Mag.* **33** 92
Silberstein L 1917 *Phil. Mag.* **33** 215
[22] Birge R R 1980 *J. Chem. Phys.* **72** 5312
[23] Thole B T 1981 *Chem. Phys.* **59** 341
[24] Birge R R, Schick G A and Bocian D F 1983 *J. Chem. Phys.* **79** 2256
[25] Jensen L, Åstrand P-O, Sylvester-Hvid K O and Mikkelsen K V 2000 *J. Phys. Chem.* A **104** 1563
[26] Jensen L, Åstrand P-O, Osted A, Kongsted J and Mikkelsen K V 2002 *J. Chem. Phys.* **116** 4001
[27] Langlet R, Arab M, Picaud F, Devel M and Girardet C 2004 *J. Chem. Phys.* **121** 9655
[28] Olson M L and Sundberg K R 1978 *J. Chem. Phys.* **69** 5400
[29] Applequist J 1993 *J. Phys. Chem.* **97** 6016
[30] Shanker B and Applequist J 1994 *J. Phys. Chem.* **98** 6486
[31] Shanker B and Applequist J 1996 *J. Chem. Phys.* **104** 6109
[32] Stern H A, Kaminski G A, Banks J L, Zhou R, Berne B J and Friesner R A 1999 *J. Phys. Chem.* B **103** 4730
[33] Jensen L, Åstrand P-O and Mikkelsen K V 2001 *Int. J. Quantum Chem.* **84** 513
[34] Mayer A 2005 *Appl. Phys. Lett.* **86** 153110
[35] Mayer A 2005 *Phys. Rev.* B **71** 235333
[36] Mayer A, Lambin Ph and Langlet R 2006 *Appl. Phys. Lett.* **89** 063117
[37] Mayer A 2007 *Phys. Rev.* B **75** 045407
[38] Mayer A and Astrand P-O 2008 *J. Phys. Chem.* A **112** 1277
[39] Wang Z and Devel M 2007 *Phys. Rev.* B **76** 195434
[40] Jensen L L and Jensen L 2008 *J. Phys. Chem.* C **112** 15697
[41] DeVoe H 1965 *J. Chem. Phys.* **43** 3199
[42] Applequist J, Sundberg K R, Olson M L and Weiss L C 1979 *J. Chem. Phys.* **70** 1240
[43] Applequist J 2000 *J. Phys. Chem.* A **104** 7133
[44] Mayer A, Lambin Ph and Astrand P-O 2008 *Nanotechnology* **19** 025203
[45] Mayer A, Gonzalez A, Aikens C M and Schatz G C 2009 *Nanotechnology* **20** 195204
[46] Fleischman M, Hendra P J and McQuillan A J 1974 *J. Chem. Phys. Lett.* **26** 163
[47] Jeanmaire D L and Van Duyne R P 1974 *J. Electroanal. Chem.* **84** 1
[48] Albrecht M G and Creighton J A 1977 *J. Am. Chem. Soc.* **99** 5215
[49] Nie S M and Emory S R 1997 *Science* **275** 1102
[50] Zhao L L, Jensen L and Schatz G C 2006 *Nano Lett.* **6** 1229
[51] Zhao L L, Jensen L and Schatz G C 2006 *J. Am. Chem. Soc.* **128** 2911
[52] Aikens C M and Schatz G C 2006 *J. Phys. Chem.* A **110** 13317
[53] Jensen L, Zhao L L and Schatz G C 2007 *J. Chem. Phys.* C **111** 4756
[54] Jensen L, Aikens C M and Schatz G C 2008 *Chem. Soc. Rev.* **37** 1061
[55] Camden J P, Dieringer J A, Wang Y, Masiello D J, Marks L D, Schatz G C and Van Duyne R P 2008 *J. Am. Chem. Soc.* **130** 12616
[56] Arfken G B and Weber H J 1995 *Mathematical Methods for Physics* 4th edn (New York: Academic) chapter 17, pp 952–91
[57] The software used for these simulations is available at http://perso.fundp.ac.be/~amayer/DCDA